

Research Article

The Selection of Anode and Cathode Materials for Top Emission Organic Light-Emitting Diodes

Fuh-Shyang Juang,¹ Krishn Das Patel ,¹ Kuo-Chun Huang,¹ Wen-Xaing Juang,¹ Jeng-Yue Chen,² and Lin-Ann Hong¹

¹Department of Electro-Optical Engineering, National Formosa University, Huwei, Yunlin 632, Taiwan

²Department of Electrical Engineering, National Formosa University, Huwei, Yunlin 632, Taiwan

Correspondence should be addressed to Krishn Das Patel; d0977108@gm.nfu.edu.tw

Received 24 September 2021; Accepted 6 June 2022; Published 21 June 2022

Academic Editor: Alberto Álvarez-Gallegos

Copyright © 2022 Fuh-Shyang Juang et al. This is an open access article distributed under the Creative Commons Attribution License, which permits unrestricted use, distribution, and reproduction in any medium, provided the original work is properly cited.

In this study top emission organic light-emitting diodes (TE-OLED) were successfully fabricated on flexible PET/multilayer disordered silver nanonetwork (MDSN) substrate with conventional LiF/Al as a semitransparent cathode and Ag as a reflective anode. The effects of the hole injection layer, anode buffer layer, and an electron injection layer on the luminescence characteristics of TE-OLEDs were investigated. At first, the thickness of cathode Al is adjusted based upon the overall transmittance of the top-emission cathode and its conductivity. There is a high energy barrier for the hole between the work function of the anode Ag (4.2 eV) and the NPB highest occupied molecular orbital (HOMO) energy level (5.5 eV), which is not favorable for hole injection. This study tested four types of hole injection layer (HIL) materials. Finally, MoO₃ was selected as an optimal HIL material, and the optimum thickness was adjusted, enabling the hole to be injected smoothly from the anode to the NPB and then to an emitting layer. The TE-OLED luminance reached 268 cd/m². There is a high energy barrier between the work function of Ag and MoO₃ HOMO (5.3 eV)—about 1.1 eV—which is still not conducive to the hole injection, so a thin layer of high work function metal Au (work function 5.1 eV) was added to the top of the anode silver, which more matches with the MoO₃ energy level. It can make the hole easier to inject from the anode to MoO₃ (HIL) and protect the silver from oxidation. At 8 V, the luminance is increased to 413.7 cd/m², and the current efficiency is 0.81 cd/A. The luminance is significantly improved. An electron transport/hole blocking layer TPBi (10 nm) was added to enhance the electron transport capability and effectively block the holes with higher electron mobility and a higher HOMO energy level of TPBi. So that more holes can remain in the emitting layer and increase the chance of the electron-hole recombination to improve the luminance and current efficiency of TE-OLED. At 8 V, the luminance and current efficiency can reach 611.4 cd/m² and 0.95 cd/A, respectively.

1. Introduction

The device structure of the organic light-emitting diode (OLED) consists of very thin films suitable for displays and lighting. The process is relatively simple. In 2020, both Samsung and Huawei launched foldable phones: the Samsung Galaxy Z Flip and the Huawei Mate X, respectively. Although there are still many problems to overcome, it is believed that foldable phones will become a new trend.

In the bottom of active-matrix organic light-emitting diode (AMOLED) display substrate, each pixel must first be prepared with an integrated circuit (IC), such as thin-film transistors (TFT) and capacitors, so if the OLED emits the light from the bottom side, the light will be blocked by the TFT and metal circuit on the substrate, meaning the actual emitting area is limited, affecting the ratio of the emitting/TFT area (i.e., aperture ratio). To improve the aperture ratio, many products in recent years have been changed to

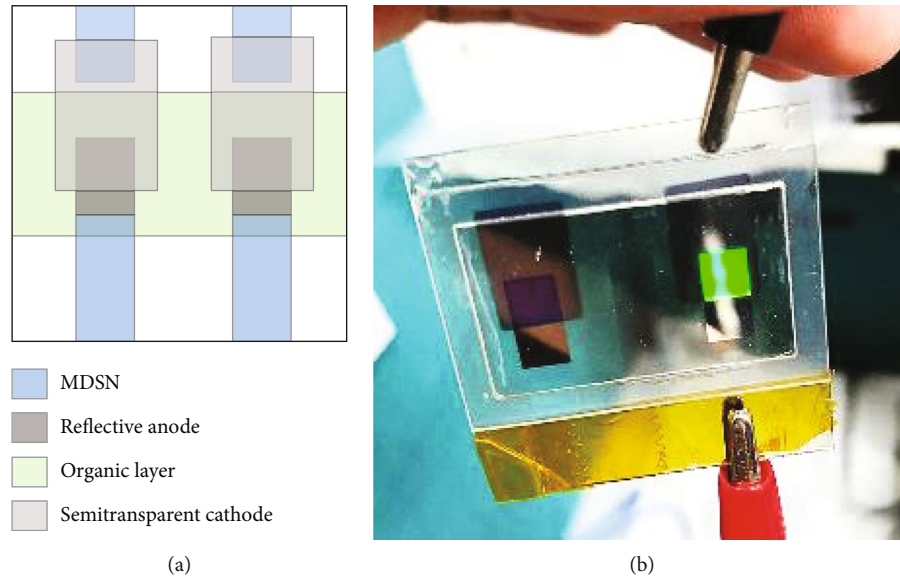


FIGURE 1: (a) Device patterns and (b) emission photo of TE-OLED with encapsulation.

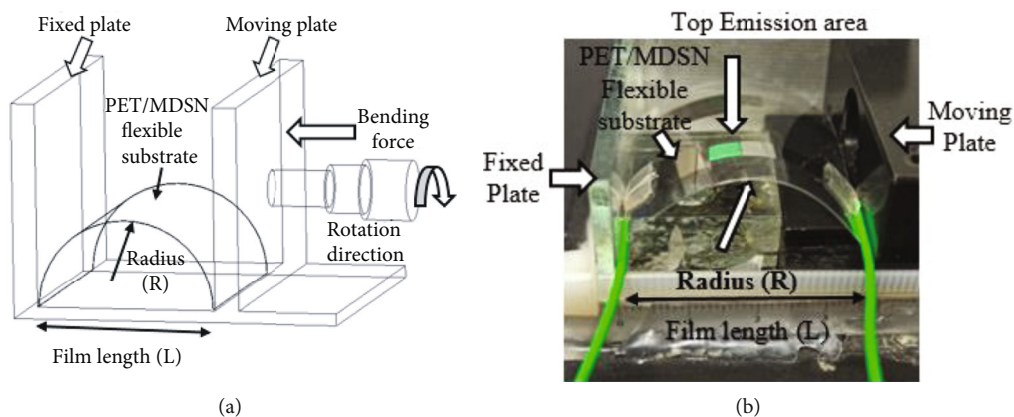


FIGURE 2: (a) Flexibility test equipment and (b) PET/MDSN substrate flexibility test.

“top emission” formats, whereby light is emitted from the cathode, rather than from the anode. For top emission OLED (TEOLED), the light does not pass through the substrate but emits from the other side, so it will not be blocked by the bottom TFT and metal circuit [1].

For flexible devices, indium tin oxide (ITO) films are not suitable as electrodes because the ITO material is brittle [2] and easily cracks or breaks when the ITO is bent several times on the flexible substrate [3]. It is not easy to reduce the resistance value of ITO film [2]. Indium metal is a rare mineral, so some new materials have been created to replace ITO. Silver nanowire (AgNW) films are inexpensive to produce, have high transmittance, high electrical conductivity, and good flexibility, and have great potential to be used on flexible substrates [4, 5, 6]. But there are still some disadvantages of AgNWs, such as low adhesion force to the substrate and low corrosion resistance.

The fabrication of semitransparent cathodes for TEOLED has been reported in the literature: Song et al.

show transparent 14 nm Ag: Al (Ag atomic dopant 4%) cathodes with a transmittance at 520 nm of 83.5% and a sheet resistance as low as $7.0 \Omega/\square$ [7]. Chang et al. show the composition of 3 nm Al and 10 nm Ag with a transmittance of 56% and a sheet resistance of $11 \Omega/\square$ for semitransparent cathodes [8]. Park et al. show Ag:60% MoO_3 (30 nm) with a transmittance of 65.9% and sheet resistance of $12.7 \Omega/\square$ [9].

Regarding the reflective anode metal and hole injection layer, Park et al. show an anode structure of silk substrate/Ag (80 nm)/ MoO_3 (4 nm), where the MoO_3 was introduced to the interface between anode and organic layer to improve the hole injection efficiency [10]. Yin et al. report a reflective anode of Ag (100 nm)/ MoO_3 (3 nm) on a glass substrate, and TEOLED was fabricated [11]. Chang et al. report a reflective anode of Al (100 nm)/ MoO_3 (2 nm) on glass. The MoO_3 layer is treated by UV-ozone; then, PEDOT:PSS is spin-coated onto the MoO_3 layer as the hole injection layer [8]. Xiaoxiao et al. used graphene/PEDOT: PSS: DMSO

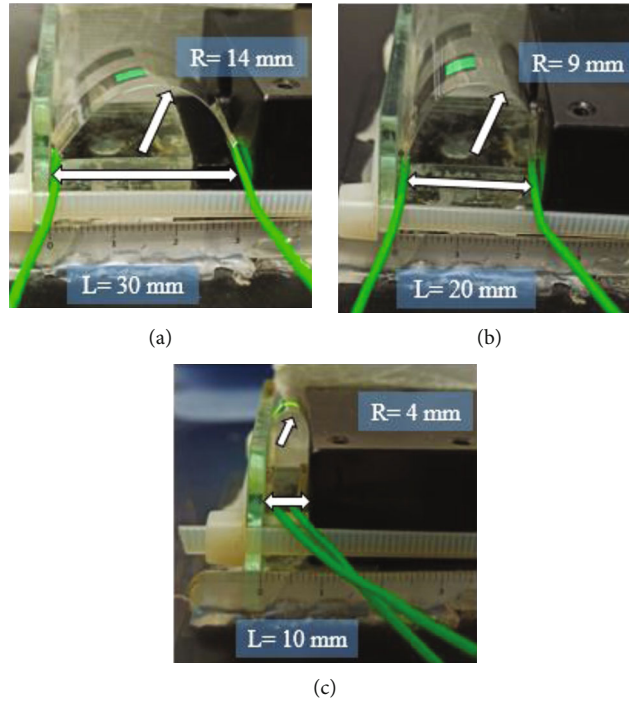


FIGURE 3: Flexibility test of TE-OLED substrates at a length of (a) $L = 30$ mm, (b) $L = 20$ mm, and (c) 10 mm.

TABLE 1: The conductivity and transmittance of Al with different thicknesses.

Al (nm)	Conductivity ($\Omega^{-1}\cdot\text{cm}^{-1}$)	Transmittance at 510 nm
10	0.42×10^4	25.7%
15	1.15×10^4	20.6%
20	1.73×10^4	8.1%

(dimethyl sulfoxide) as an anode on PET substrate, and a bottom emission OLED was fabricated [12]. By Shang-Yu et al., the photoresist was coated on flexible stainless-steel substrate, and then, Ag/ WO_3 was employed as an anode, and the top emission OLED was fabricated [13].

The flexible substrate used in this study is a multilayer disordered silver nanonetwork (MDSN) transparent film fabricated with a sputtering physical vapour deposition system on PET substrate, purchased from ConvergeEver INC., LTD, Taiwan. This MDSN flexible substrate is resistant to electromagnetic interference (EMI). It can be applied to large size touch displays, curved touch, OLED lighting, colour changing windows, transparent displays, LCD, electronic paper, active capacitive pen precision touch panel transparent heating panels, etc. MDSN has UV-weather resistance and low silver migration characteristics. The raw material cost is also lower and competitive in the field of flexible substrates.

In this study, a top-emission organic light-emitting diode (TE-OLED) of an area of $5 \text{ mm} \times 5 \text{ mm}$ was fabricated by full thermal vacuum deposition on PET/MDSN substrate

using high reflectivity metal Ag as the anode and semitransmissive Al as the cathode.

2. Experiments

The anode and cathode patterns of the TE-OLED were designed using AutoCAD software, and the electrode area was carved on PET/MDSN (thickness $125 \mu\text{m}$, sheet resistance $10.85 \Omega/\square$) flexible substrate using a laser engraving machine. The substrates were soaked in acetone, isopropanol, and deionized water for 20 minutes each using an ultrasonic cleaner. The substrate was then blown dry with a nitrogen gun (N_2) and baked in an oven at 80°C for 10 minutes. Next, organic and metallic layers were deposited by a thermal vacuum deposition system (at vacuum pressure 6×10^{-6} torr). The reflective anode was deposited with Ag/Au/ MoO_3 . The organic materials are the hole transport layer (HTL) NPB, the electron transport layer (ETL)/emitting layer Alq_3 , and the ETL/hole blocking layer (HBL) TPBi. The transparent cathode is LiF with a thickness of 0.8 nm and aluminium with a thickness of 15 nm. The device patterns and emission photos of the TE-OLED are shown in Figures 1(a) and 1(b), respectively. The luminous area is $5 \text{ mm} \times 5 \text{ mm}$. Finally, a Keithley 2400 (power supply) was used to provide bias to the TE-OLED, and a Spectra Scan PR 650 Spectra Colorimeter was used to measure the luminance and spectra to obtain current-luminance-voltage characteristic curves.

2.1. Device Flexibility Test. Using the flexibility measurement equipment, the flexibility of the top emission OLEDs was measured by placing a flexible PET/MDSN substrate

TABLE 2: Device parameters with different hole injection materials (unit: nm).

Anode	HIL	HTL	EML	EIL	Cathode
Ag	Materials/thickness	NPB	Alq3	LiF	Al
	TFB (solved in chlorobenzene)	30			
80	Poly-TPD (solved in chlorobenzene)	30	35	60	0.8
	PEDOT:PSS	25			15
	MoO ₃	2			

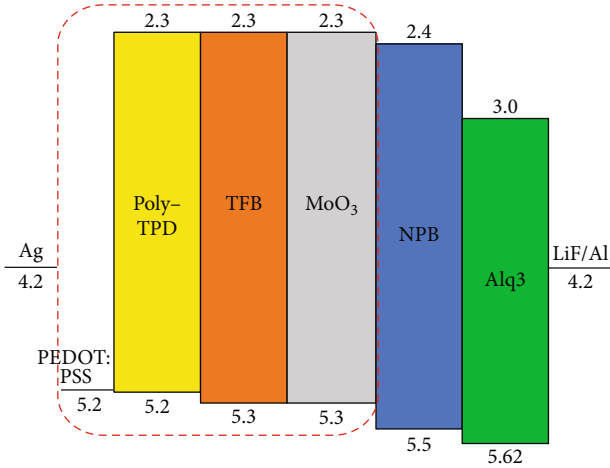


FIGURE 4: Energy band diagram for TE-OLEDs with different hole injection materials.

between a fixed plate and a moving plate, as shown in Figures 2(a) and 2(b).

In order to evaluate the flexibility of the TE-OLED, a bending force was applied in one direction, and the bending test was conducted at the constant voltage of 5 V. Figures 3(a)–3(c) illustrate the measured PET/MDSN substrate flexibility in lengths of 30 mm, 20 mm, and 10 mm. Based on this measurement, it is determined that the TE-OLED on PET/MDSN substrate is able to sustain at the extreme bending radius of 4 mm.

3. Results and Discussion

In the top emission OLED structure, the transparent cathode has the most important impact on the efficiency of the devices. When the Al is thicker, its conductivity is higher, but the transmittance is lower, which affects the light emitting output. When the Al is thinned, the transmittance increases, but the conductivity decreases. In this study, aluminium is used as the cathode metal to investigate the effect of the thickness of aluminium on its transmittance and conductivity. As shown in Table 1, the conductivity was measured using a Hall measurement system for different Al thicknesses. For Al thickness of 20 nm, the conductivity is high, but the transmittance is only 8.1%. Thickening of Al leads to a decrease in transmittance, so Al 15 nm has a good conductivity and sufficient transmittance as a transparent cathode for top emission OLED.

In this study, TE-OLED uses PET/MDSN as the substrate with an MDSN sheet resistance of $10.85 \Omega/\square$ (purchased from ConvergeEver Co., LTD), and Ag is deposited on top of MDSN as the reflective anode (thickness 80 nm). The energy barrier between Ag and NPB HOMO is about 1.3 eV. For the holes to be injected smoothly into the emitting layer from the anode, the appropriate hole injection material must be selected. The structure of the TE-OLED for the HIL material study was PEN/MDSN/Ag (80 nm)/X/ NPB (35 nm)/Alq₃ (60 nm)/LiF (0.8 nm)/Al (15 nm) where four materials were chosen for the X-layer: MoO₃ (by evaporation), PEDOT: PSS (by spin-coating), TFB (solved in chlorobenzene then spin-coating), and Poly-TPD (solved in chlorobenzene then spin-coating). The parameters of each layer are shown in Table 2, exploring the effects of different HIL materials on the luminous characteristics of TE-OLEDs. The energy band diagram is shown in Figure 4. The obtained characteristics are shown in Figure 5(a) current density-voltage curve and Figure 5(b) luminance-voltage curve.

From Figures 5(a) and 5(b), it can be seen that the hole injection effect of TFB, Poly-TPD, and PEDOT: PSS as HIL is not good enough using the spin-coating method. As TFB and poly-TPD are organic materials, conductivity is poor, rendering the hole insufficient to inject into the light-emitting layer so the current density is low. PEDOT: PSS film has good conductivity, so some of the holes can still be injected into the emitting layer to make the device emit light slightly, as shown in Figure 5(b). The thermal vacuum evaporation technique can control the MoO₃ thickness to 1–5 nm for optimal hole injection from MoO₃ into NPB (high current density and high luminance) [8, 12, 14, 16]. MoO₃ behaves as an anode buffer in the OLEDs [17, 18].

Next, the repercussions of MoO₃ HIL thickness on the luminescence characteristics were discussed. Although the reflectivity of the anode metal Ag is over 80%, the Ag work function is only 4.2 eV, and the energy barrier of 1.3 eV is formed between Ag and NPB HOMO energy levels. To reduce this energy barrier to increase the number of holes injected into the emitting layer by the anode, another layer of MoO₃ (HOMO 5.3 eV) is deposited on top of the anode Ag metal, and the energy barrier between MoO₃/NPB HOMO is only about 0.2 eV, which is expected to enhance the hole injection amount. Many experts and researchers have used MoO₃ as a HIL or anode buffer layer for top emission OLED (TEOLED) [8, 12, 14–19]. The structure of the TE-OLED is PEN/MDSN/Ag (80 nm)/MoO₃ (x nm)/NPB (35 nm)/Alq₃ (65 nm)/LiF (0.8 nm)/Al (15 nm). The energy band diagram is shown in Figure 6(a), in which the MoO₃ thickness is adjusted to 1, 2, and 5 nm, respectively.

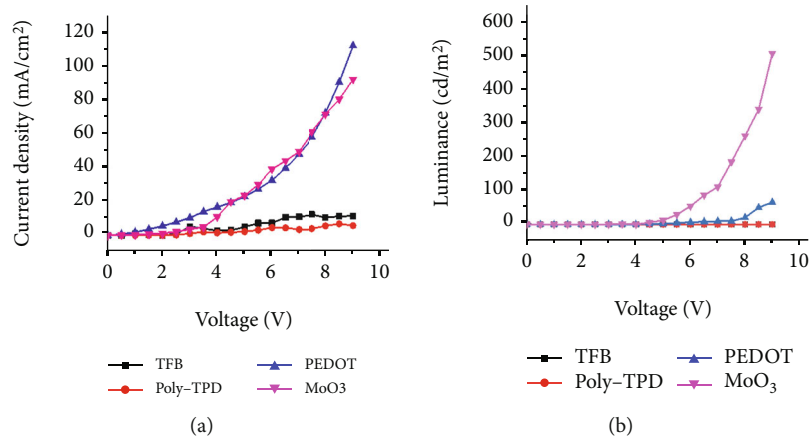


FIGURE 5: (a) Current density-voltage curves and (b) luminance-voltage curves of TE-OLED with various hole injection materials compared.

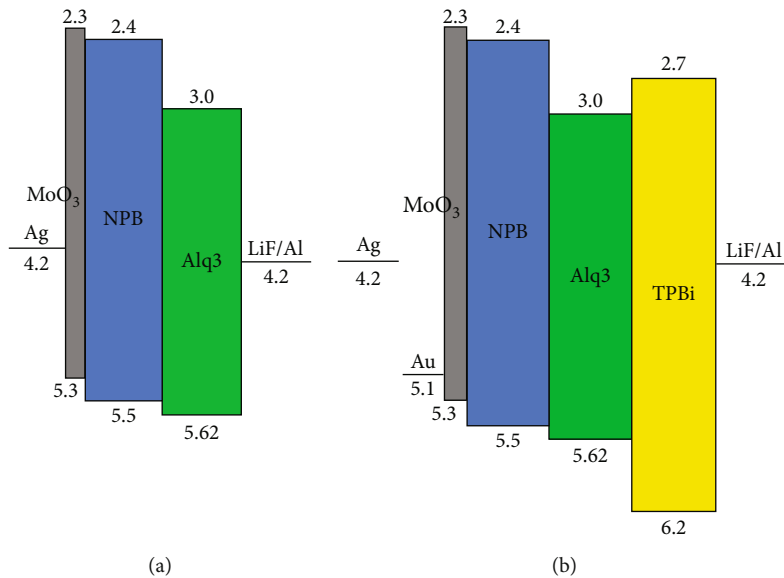


FIGURE 6: (a) TE-OLED energy level diagram with MoO₃ thickness adjustment and (b) TE-OLED energy level of adding Au/MoO₃ on the anode side and TPBi on the cathode side.

Figure 7 shows the current density-luminance-voltage curves of the structure, and Figure 8 shows the current efficient-voltage curves of the structure.

Compared with Ag/NPB, the Ag/MoO₃/NPB anode structure with a lower energy barrier between MoO₃/NPB HOMO results in holes that can be easily injected from Ag to NPB. When the device is biased, part of the applied voltage (V) is divided to the anode side to make holes inject into NPB and transport to Alq₃, and part of the applied voltage is divided to the cathode side to make electrons inject into Alq₃ so that the holes and electrons can recombine in the emitting layer to emit the light. Figure 7 shows the current density-luminance-voltage curves for FET-OLED with Ag/MoO₃/NPB anode structure. When the MoO₃ thickness is 1 nm, the hole injection current is still low, resulting in a weaker luminance. When the MoO₃ thickness increases to 2 nm, the current density increased slightly higher than that of

1 nm. The current density is 71.64 mA/cm² at 8 V, and the luminance increased significantly at 7-9 V. As shown in Figure 7, the luminance is 268.4 cd/m² at 8 V, and the current efficiency is 0.37 cd/A. When the thickness of MoO₃ increases to 5 nm, the current density increases sharply to 122.75 mA/cm² at 8 V. There are some possibilities: (1) more applied voltage is across the anode side (when compared with that of MoO₃ 1 nm), resulting in a greater increase in the number of holes injected. (2) The thicker MoO₃ layer may generate more defects in the Ag/MoO₃/NPB interface which results in leakage current in the anode side.

Although the number of holes increases, the quantity of electrons does not increase (as the partial voltage at the cathode side is less), which fails to reach equilibrium (balance) so that the luminance decreases dramatically. The luminance was about 107 cd/m² at 8 V, and the current efficiency decreased to 0.09 cd/A. In conclusion, a thickness of MoO₃

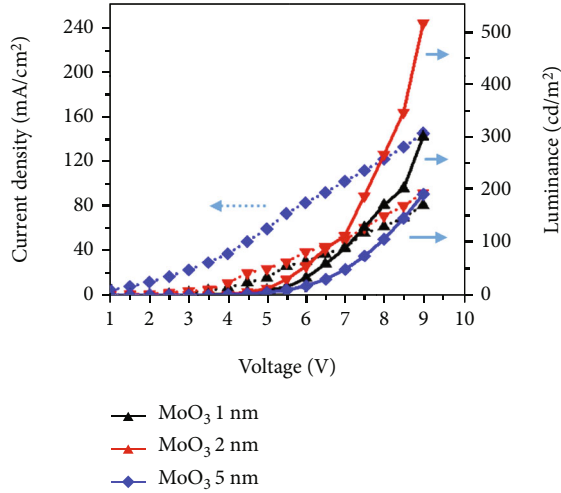


FIGURE 7: Current density-luminance-voltage curves of TE-OLED with the MoO_3 thickness adjusted.

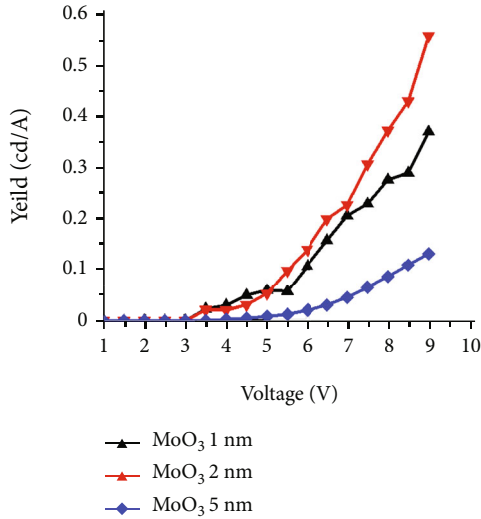


FIGURE 8: TE-OLED current efficiency-voltage characteristic curve with variable MoO_3 thickness.

of 2 nm is the most appropriate one as the luminance and efficiency are the highest.

From the current density-voltage curves in Figure 7, another phenomenon can be found: the current density-voltage characteristics of TE-OLEDs with an Ag/MoO_3 anode structure tend to have ohmic contact characteristics. This may be caused by the uneven surface of Ag/MoO_3 or the existence of some defects in the $\text{Ag}/\text{MoO}_3/\text{NPB}$ interface which generate leakage current in the anode side. The thicker the MoO_3 layer, the higher the current density, especially with MoO_3 5 nm. This can be improved after inserting an Au layer as discussed below.

Since the energy barrier between Ag/MoO_3 is still larger (about 1.1 eV), the hole is not easily injected into MoO_3 , so a metal with a higher work function than Ag is required. The problem of the Al/MoO_3 interface with leakage current also

TABLE 3: Variable TE-OLED structure parameters for each layer thickness (unit: nm).

No	Anode Ag	Au	HIL MoO_3	HTL NPB	EML Alq_3	ETL TPBi	EIL LiF	Cathode Al
A			1					
B	80	—	2	35	60	—		
C			5				0.8	15
H	80	3	2	35	60	—		
I					55	10		

needs to be solved. In this study, a thin layer of Au (3 nm thick, work function 5.1 eV) is added between the $\text{Ag}-\text{MoO}_3$ to make the hole injection step from Ag into MoO_3 become smoother, as shown in the anode part of the band diagram in Figure 6(b). The Au on the Ag surface can also prevent the degradation of Ag film conductivity caused by the oxidation of Ag in the atmosphere, thus enhancing the luminous efficiency of TE-OLED. The device structure is $\text{PEN}/\text{MDSN}/\text{Ag}$ (80 nm)/Au (3 nm)/ MoO_3 (2 nm)/NPB (35 nm)/ Alq_3 (60 nm)/LiF (0.8 nm)/Al (15 nm). The device parameters are listed in Table 3. Figures 9(a) and 9(b) show the current density-luminance-voltage and current efficiency-voltage characteristics of TE-OLED with $\text{Ag}/\text{Au}/\text{MoO}_3$ structure, respectively.

By adding a thin layer of Au on top of the anode Ag, the energy level for hole injection from Ag to MoO_3 is established like a gradual ladder, and a stable Schottky barrier is formed, as shown in the anode side of Figure 6(b). Both Ag/MoO_3 and $\text{Ag}/\text{Au}/\text{MoO}_3$ devices are compared with each other, and the thickness of the organic layer NPB/ Alq_3 remains the same for both. Equation (1) is the equation of total V applied to the OLED and result in total current density J . For $\text{Ag}/\text{MoO}_3/\text{NPB}/\text{Alq}_3/\text{LiF}/\text{Al}$ OLED, the partial voltage of $\text{Ag}-\text{MoO}_3$, NPB- Alq_3 , and LiF-Al is V_h , V_o , and V_e , respectively, similar for that of $\text{Ag}/\text{Au}/\text{MoO}_3/\text{NPB}/\text{Alq}_3/\text{LiF}/\text{Al}$. The detailed discussions are listed in Table 4.

$$V = V_h + V_o + V_e, \quad (1)$$

$$J = J_h + J_e. \quad (2)$$

Compared with the Ag/MoO_3 structure, the current density of the TE-OLED with $\text{Ag}/\text{Au}/\text{MoO}_3$ structure decreases from $71.64 \text{ mA}/\text{cm}^2$ to $51.33 \text{ mA}/\text{cm}^2$ at 8 V, but the luminance increases from $268.4 \text{ cd}/\text{m}^2$ to $413.7 \text{ cd}/\text{m}^2$ as shown in Figure 9(a). The current efficiency also increased from 0.37 to 0.81 cd/A as shown in Figure 9(b). Compared with Ag/MoO_3 , the $\text{Ag}/\text{Au}/\text{MoO}_3$ anode after 3 nm Au insertion has a more stable formation of Schottky barrier which can be observed from the I-V Schottky characteristics shown in Figure 9(a). The overall comparisons of the I-V characteristics of Ag/MoO_3 (different thicknesses) and $\text{Ag}/\text{Au}/\text{MoO}_3$ are shown in Figure 10. It is found that the cut-in voltage of the $\text{Ag}/\text{Au}/\text{MoO}_3$ device increases (to a higher value of about 4.5 V), and $dV/d(\ln(J))$ slope decreases (as deduced from the Schottky diode I-V equation), which confirms the formation of a more stable Schottky contact between Ag/

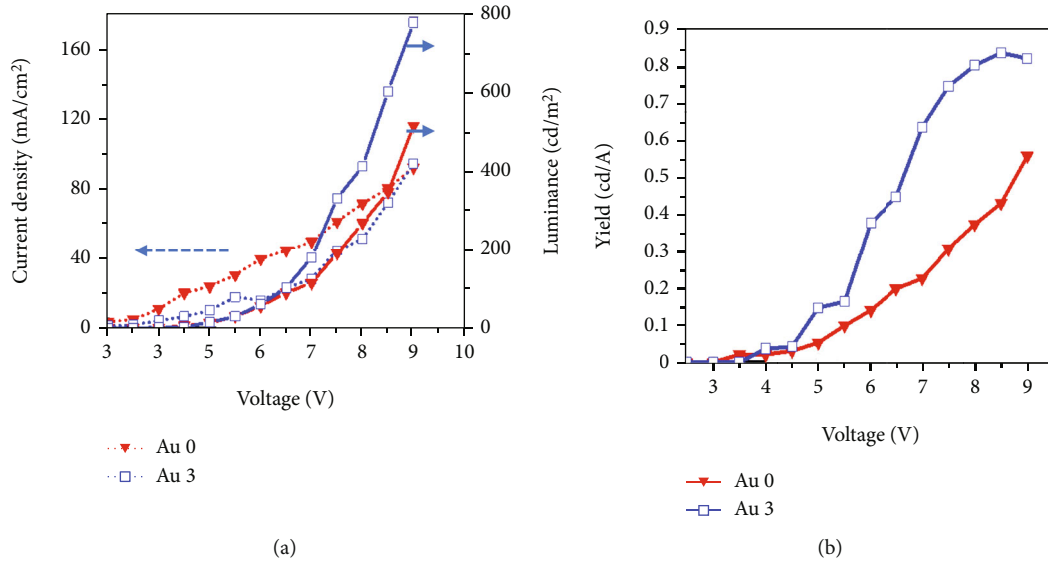


FIGURE 9: The characteristic curves of (a) current density-luminance-voltage and (b) current efficient-voltage of TE-OLED in the anode Ag/Au/MoO₃ structure.

TABLE 4: A detailed discussion of resistance, voltage, and current of anode side, an organic layer, and cathode side, respectively, in TE-OLED.

Device structure	Total	Anode side	Organic layer	Cathode side Alq/LiF/Al	I-L-V results
Ag/NPB w/o MoO ₃	R= V= I= R=	R _h (high) (due to high barrier) V _h (high, V _h > V _e) I _h (low) R _h (low)	R _o V _o R _o	R _e (low) V _e (low) I _e (low) R _e (low)	No emitting No h ⁺ crt Low crt
Ag/MoO ₃ vs w/o MoO ₃	V= I= R=	1. Ag/MoO ₃ /NPB barrier decreased. 2. IV curves like ohmic contact. 3. Ag/MoO ₃ interface may have defects. V _h (decreased a little) (transferred to cathode) I _h (high, I _h > I _e) R _h (increased)	V _o R _o	V _e (increased) I _e (increased) R _e (low)	Emitting, total current increased
Ag/Au/MoO ₃ vs Ag/MoO ₃	V= I= R=	1. Schottky barrier formed and energy level for h ⁺ injection likes a gradual ladder. 2. Ag/MoO ₃ interface improved. V _h I _h (decreased more) e/h current more balanced R _h	V _o R _o	V _e I _e (increased a little) R _e	Luminance increased, total current decreased
Ag/Au/MoO ₃ /.../TPBi/LiF/Al	V= I=	V _h I _h	Decreased due to TPBi with higher e mobility. V _o	V _e I _e (increased) e/h crt more balanced	Total current increased Luminance increased

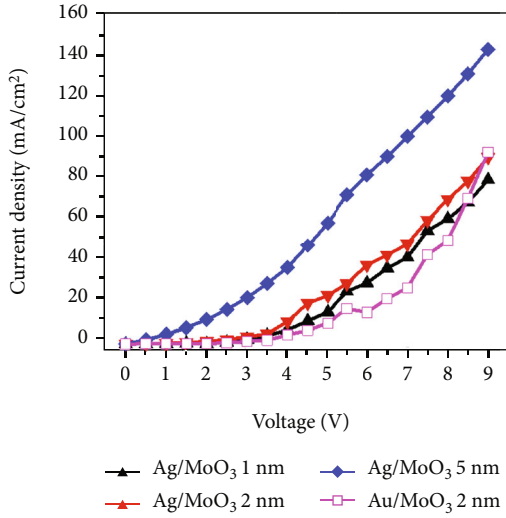


FIGURE 10: Overall comparison of I-V properties of Ag/MoO₃ (different thicknesses) with Ag/Au/MoO₃.

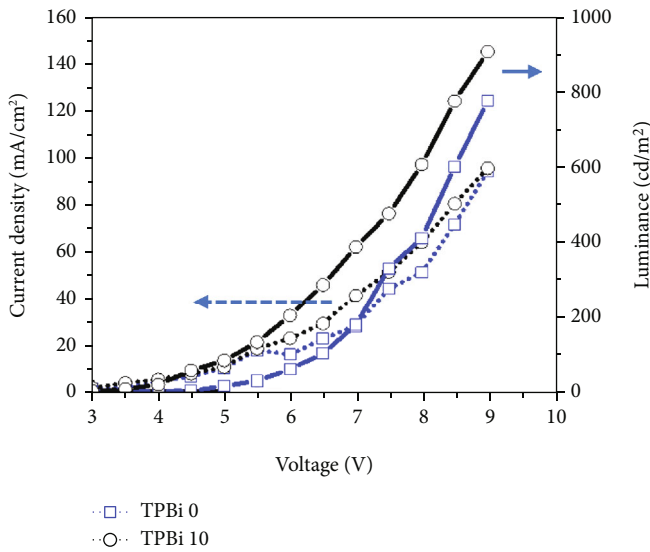


FIGURE 11: Current density-luminance-voltage characteristic curve characteristics of TE-OLED with electron transport/hole blocking layer TPBi.

Au/MoO₃/NPB. Therefore, the hole injection current (J_h in Equation (2)) at the anode side decreases due to the insertion of Au (resistance increased) and the formation of the Schottky barrier, while at the cathode side, the Alq₃/LiF/Al is a conventional structure where the electron injection remains at a general condition (compared with that of Ag/MoO₃). So the hole injection current decreases and the electron injection current (J_e in Equation (2)) increases a little which promotes the electron and hole current to be more balanced, as discussed in Table 4. So the luminance and current efficiency of the Ag/Au/MoO₃ device is enhanced compared with the Ag/MoO₃ structure, as shown in Figure 9(b). The total current density of the Ag/MoO₃ (Au 0 nm) device

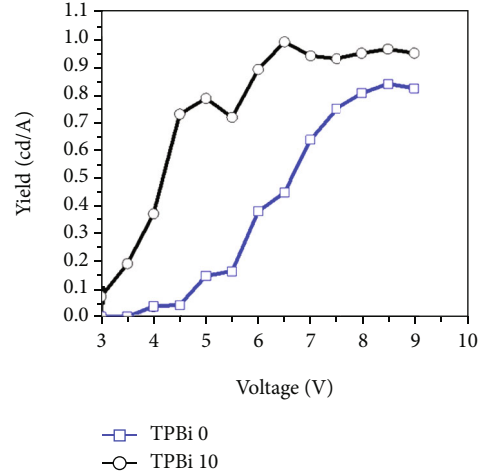


FIGURE 12: Current efficiency-voltage characteristic curves of TE-OLED with electron transport/hole blocking layer TPBi.

is larger than that of Ag/Au/MoO₃ as the dashed I-V curves shown in Figure 9(a). It is also confirmed that the interface between Ag/MoO₃/NPB is more unstable (non Schottky) and prone to current leakage if no Au is inserted between Ag and MoO₃.

Although the luminescent layer Alq₃ has electron-transport property, its electron mobility is low (about $8.0 \times 10^{-6} \text{ cm}^2/\text{V}\cdot\text{s}$), which is not conducive to electron transport. Therefore, another electron transport layer TPBi with high electron mobility ($6.5 \times 10^{-5} \text{ cm}^2/\text{V}\cdot\text{s}$) is added between Alq₃ and the cathode to accelerate the electron transport rate. The structure of the device is PEN/MDSN/Ag (80 nm)/Au (3 nm)/MoO₃ (2 nm)/NPB (35 nm)/Alq₃ (55 nm)/TPBi (10 nm)/LiF (0.8 nm)/Al (15 nm), and the thicknesses of each layer of the TE-OLED are listed in Table 3. Figure 11 shows the current density-luminance-voltage characteristic curves when inserting the electron transport layer/hole blocking layer (TPBi).

Figure 12 shows the current efficiency-voltage characteristics curves. After adding a layer of 10 nm TPBi to the TE-OLED, the current density increases from $51.33 \text{ mA}/\text{cm}^2$ to $64.29 \text{ mA}/\text{cm}^2$ at 8 V. The luminance also increases from $413.7 \text{ cd}/\text{m}^2$ to $611.4 \text{ cd}/\text{m}^2$ and the current efficiency from $0.81 \text{ cd}/\text{A}$ to $0.95 \text{ cd}/\text{A}$.

TPBi not only has the role of accelerating electron transportation (lead to organic layer equivalent resistance reduced) but also its high HOMO energy level (higher than Alq₃) can be used as a hole blocking layer. As shown in the energy band diagram in Figure 6(b), TPBi can block the holes and prevent them from rapidly flowing away from Alq₃ (emitting layer) to the cathode. So the holes could be confined in the emitting layer, increasing the chance of electron-hole recombination and increasing the luminance of TE-OLED.

In this study, the I-L-V characteristics of four TE-OLED structures, Ag anode without MoO₃, Ag/MoO₃, Ag/Au/MoO₃, and Ag/Au/MoO₃/.../TPBi/LiF/Al, were analyzed. The details of correlative variation of resistance, partial

voltage, and electron/hole injection current between the anode, organic layer, and cathode are explained in Table 4.

4. Conclusions

In this study, we successfully fabricated top-emitting OLEDs (TE-OLEDs) on a flexible PET/MDSN substrate with conventional LiF/Al as the cathode and Ag as the reflective anode. For the cathode to be transparent and have good conductivity, the thickness of Al was thinned to 15 nm, with a transmittance of 20.6% at 510 nm and conductivity of 1.15×10^4 ($\Omega^{-1}\cdot\text{cm}^{-1}$). The thicker the Al, the higher the conductivity, but the transmittance is relatively lower, and the luminance decreases. An optimum thickness of 15 nm of Al was obtained from this experiment.

Silver with high reflectivity is suitable as a reflective anode (thickness of 80 nm), but for the hole, there is a high energy barrier (about 1.3 eV) between the work function of Ag and the NPB HOMO, which is not favorable for hole injection. In this study, MoO₃ was selected from several HIL materials as the best one. The optimum thickness of MoO₃ of 2 nm was determined, which can make the hole inject smoothly from the anode to NPB and then into the emitting layer. The luminance of TE-OLED with Ag/MoO₃ anode is 268 cd/m². PEDOT: PSS can also help the hole inject into NPB, but its luminance is much lower than that of MoO₃.

The work function 4.2 eV of Ag and the HOMO of MoO₃ still have a large energy barrier—about 1.1 eV—which is still not conducive to hole injection. Therefore, a layer of high work function metal—Au 3 nm—is added on top of the anode silver. Since the work function of Au 5.1 eV more matches with the HOMO of MoO₃, it is easier for the hole to inject from the anode to MoO₃ (HIL), which reduces the driving voltage and protects the silver from oxidation, improving the Ag/MoO₃/NPB interface. At 8 V, the current density, luminance and current efficiency reach 51.33 mA/cm², 413.7 cd/m² and 0.81 cd/A, respectively. The characteristics are significantly improved.

Finally, a layer of electron transport and hole blocking TPBi (10 nm) is inserted to enhance the electron transport ability and effectively block the hole with the higher electron mobility and higher HOMO of TPBi, so that more holes remain in the emitting layer and increase the chance of the electron-hole recombination to improve the luminance and efficiency of TE-OLED. The current density, luminance, and current efficiency can reach 64.29 mA/cm², 611.4 cd/m², and 0.95 cd/A at 8 V, respectively. The top emission OLEDs were successfully fabricated on PET/MDSN substrate, and their luminance characteristics were enhanced by improving the anode material, choosing the best hole injection material, and inserting a higher electron mobility ETL. The TE-OLEDs were also tested for flexibility during this study, and the device performance did not degrade with an extreme bending curvature radius of 4 mm.

Data Availability

The data used to support the findings of this study are included within the article.

Conflicts of Interest

The authors declare that they have no conflicts of interest.

Acknowledgments

The authors gratefully acknowledge the financial support provided by the Ministry of Science and Technology (MOST), Taiwan, under grant numbers MOST-109-2221-E-150-014 and MOST-110-2221-E-150-013.

References

- [1] S. Shang-Yu, *Study of Top-Emitting Organic Light Emitting Diodes on Flexible Substrate [Master Thesis]*, Institute of Display Technology, National Chiao Tung University, Taiwan, 2009.
- [2] S. H. Kim, "Influence of surface roughness on the efficiency of a flexible organic solar cell," *Journal of Ceramic Processing Research*, vol. 21, no. 1, pp. 42–49, 2020.
- [3] C. Lee, R. Pandey, B. Wang, W. Choi, D. Choi, and Y.-J. Oh, "Nano-sized indium-free MTO/Ag/MTO transparent conducting electrode prepared by RF sputtering at room temperature for organic photovoltaic cells," *Solar Energy Materials & Solar Cells*, vol. 132, pp. 80–85, 2015.
- [4] B. Y. Wang, E. Lee, Y. J. Oh, and H. W. Kang, "A silver nanowire mesh overcoated protection layer with graphene oxide as a transparent electrode for flexible organic solar cells," *RSC Advances*, vol. 7, no. 83, pp. 52914–52922, 2017.
- [5] W.-Y. Hsu, *The Study on the Electro-Optical Properties and OLED Applications of Silver Nanowire Thin Films [Master Thesis]*, Chung Yuan Christian University, Taiwan, 2014.
- [6] W. Li, H. Zhang, S. Shi et al., "Recent progress in silver nanowire networks for flexible organic electronics," *Journal of Materials Chemistry C*, vol. 8, pp. 4636–4674, 2020.
- [7] M.-G. Song, K.-S. Kim, H. I. Yang et al., "Highly reliable and transparent Al doped Ag cathode fabricated using thermal evaporation for transparent OLED applications," *Organic Electronics*, vol. 76, article 105418, 2020.
- [8] H.-W. Chang, H.-F. Meng, S.-F. Horng, and H.-W. Zan, "ITO-free large-area top-emission organic light-emitting diode by blade coating," *Synthetic Metals*, vol. 212, pp. 19–24, 2016.
- [9] M.-J. Park, S. K. Kim, R. Pode, and J. H. Kwon, "Low absorption semi-transparent cathode for micro-cavity top-emitting organic light emitting diodes," *Organic Electronics*, vol. 52, pp. 153–158, 2018.
- [10] Y.-F. Liu, M.-H. An, Y.-G. Bi, D. Yin, J. Feng, and H.-B. Sun, "Flexible efficient top-emitting organic light-emitting devices on a silk substrate," *IEEE Photonics Journal*, vol. 9, no. 5, pp. 1–6, 2017.
- [11] M. Yin, Y. Ziwei, T. Pan et al., "Efficient and angle-stable white top-emitting organic light emitting devices with patterned quantum dots down-conversion films," *Organic Electronics*, vol. 56, pp. 46–50, 2018.
- [12] W. Xiaoxiao, F. Li, W. Wei, and T. Guo, "Flexible organic light emitting diodes based on double-layered graphene/PEDOT:PSS conductive film formed by spray-coating," *Vacuum*, vol. 101, pp. 53–56, 2014.
- [13] S. Shang-Yu, M.-H. Ho, P.-Y. Kao et al., "Efficient p-i-n top-emitting flexible organic light emitting diodes on planarized

- stainless steel foil," *SID 09 DIGEST*, vol. 40, no. 1, pp. 1524–1527, 2009.
- [14] S.-K. Kwon, E.-H. Lee, K.-S. Kim et al., "Efficient micro-cavity top emission OLED with optimized Mg:Ag ratio cathode," *Optics Express*, vol. 25, no. 24, pp. 29906–29915, 2017.
- [15] T.-H. Yeh, C.-C. Lee, C.-J. Shih, G. Kumar, S. Biring, and S.-W. Liu, "Vacuum-deposited MoO₃/Ag/WO₃ multilayered electrode for highly efficient transparent and inverted organic light-emitting diodes," *Organic Electronics*, vol. 59, pp. 266–271, 2018.
- [16] R. B. Pode, C. J. Lee, D. G. Moon, and J. I. Han, "Transparent conducting metal electrode for top emission organic light-emitting devices: Ca–Ag double layer," *Applied Physics Letters*, vol. 84, no. 23, pp. 4614–4616, 2004.
- [17] X. Haitao and X. Zhou, "Investigation of hole injection enhancement by MoO₃ buffer layer in organic light emitting diodes," *Journal of Applied Physics*, vol. 114, no. 24, p. 244505, 2013.
- [18] L. Hui, Y. Jun-sheng, and Z. Wei, "Investigation of top-emitting OLEDs using molybdenum oxide as anode buffer layer," *Optoelectronics Letters*, vol. 8, no. 3, pp. 197–200, 2012.
- [19] K. J. Reynolds, J. A. Barker, N. C. Greenham, R. H. Friend, and G. L. Frey, "Inorganic solution-processed hole-injecting and electron-blocking layers in polymer light-emitting diodes," *Journal of Applied Physics*, vol. 92, no. 12, pp. 7556–7563, 2002.